9

Densitometry

Hastings A. Smith, Jr., and Phyllis A. Russo

9.1 INTRODUCTION

The term "densitometry" refers to measurement of the density of a material by determining the degree to which that material attenuates electromagnetic radiation of a given energy. Chapter 2 details the interaction of electromagnetic radiation (specifically x rays and gamma rays) with matter. Because electromagnetic radiation interacts with atomic electrons, densitometry measurements are element-specific, not isotope-specific. Two phenomena occur during a densitometry measurement: first, part of the incident radiation energy is absorbed; and second, the ionized atoms emit characteristic x rays as they return to their stable atomic ground states. This latter process, known as x-ray fluorescence (XRF), is a powerful method for element-specific assays. (See Chapter 10 for details of the XRF technique.) In some cases, gamma-ray transmission measurements can provide information not only on the bulk density of a sample but also on its composition. Because the absorption of low-energy photons (primarily by the photoelectric effect) is a strong function of the atomic numbers (Z) of the elements in the sample, a measurable signature is provided on which an assay can be based.

This chapter describes various densitometry techniques involving measurement of photon absorption at a single energy and at multiple energies and measurement of differential photon attenuation across absorption edges. Applications using these techniques are discussed, and measurement procedures with typical performance results are described.

All densitometry measurements discussed in this chapter are based on determination of the transmission of electromagnetic radiation of a given energy by the sample material. The mathematical basis for the measurement is the exponential absorption relationship between the intensity (I_0) of photon radiation of energy (E) incident on a material and the intensity (I) that is transmitted by a thickness (x) of the material:

$$I = I_0 \exp(-\mu\rho x) \tag{9-1}$$

where ρ is the mass density of the material and μ is the mass attenuation coefficient, which is evaluated at the photon energy E. The incident and transmitted intensities are the measured quantities. Their ratio (I/I_0) is called the transmission (T) of the material at the photon energy of interest. If any two of the three quantities in the exponent expression are known from other data, the third quantity can be determined by the transmission measurement. A strong advantage of a procedure that measures photon transmissions is that the data are handled as a ratio of two similarly measured quantities, thereby removing many bothersome systematic effects that often complicate the measurement of absolute photon intensity.

The measured electromagnetic radiation can originate from an artificial x-ray source (which emits photons with a continuous energy spectrum) or from a natural gamma-ray source (which emits gamma rays with discrete energies). The sample material is placed between a photon source and a photon detector (see Figure 9.1). The transmission of the sample is determined by measuring the photon intensity of the source both with (I) and without (I_0) the sample material present.

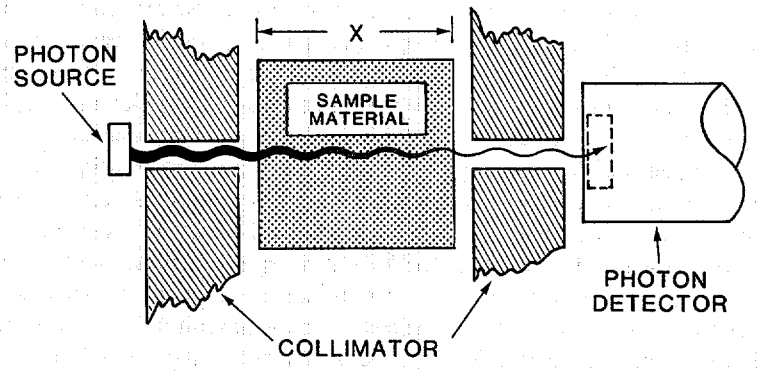

Fig. 9.1 Key components of a densitometry measurement.

9.2 SINGLE-LINE DENSITOMETRY

9.2.1 Concentration and Thickness Gauges

If a sample is composed of one type of material—or of a mixture of materials whose composition is tightly controlled except for one component—then the sample transmission at one gamma-ray energy can be used as a measure of the concentration (density ρ) of the varying component. Normally, discrete-energy gamma-ray sources are used. For example, consider a two-component system, such as a solution of uranium and nitric acid, whose components have respective densities ρ and ρ_0 and mass attenuation coefficients μ and μ_0 at a given gamma-ray energy. The natural logarithm of the photon transmission at that energy is given by

$$\ln T = -(\mu\rho + \mu_0\rho_0)x \ . \tag{9-2}$$

With ρ as the unknown concentration,

$$\rho = -\left(\frac{1}{\mu x}\right)\ln T - \frac{\mu_0\rho_0}{\mu} \ . \tag{9-3}$$

Equation 9-3 may be applied as a gauge for the concentration of an unknown amount of substance (ρ) in a known, carefully controlled solvent concentration (ρ_0).

In applying the concentration gauge to special nuclear material (SNM) solutions (uranium and plutonium), it is critical both that the mass attenuation coefficients be well characterized for the solvent (μ_0) and the SNM (μ) and that the solvent composition (ρ_0) be well known and constant from sample to sample. The sample solutions should not be vulnerable to contamination because contamination would cause variations in the effective values of ρ_0 and μ_0.

Single-line measurement can also be applied as a thickness gauge for materials of known and tightly controlled composition. On-line measurement of the transmitted photon intensity at one energy through metals and other solids in a constant measurement geometry is a direct measure of the thickness (x) of those materials. Such information is useful for timely control of some commercial production processes.

9.2.2 Measurement Precision

Consider the case of a single-line concentration measurement in which no significant fluctuations are present in the solvent composition. The measurement precision of the unknown quantity (ρ) is determined by the statistical variance of the transmission (T). The relative precision of the density measurement is obtained by differentiating Equation 9-3:

$$\frac{\sigma(\rho)}{\rho} = \left(\frac{1}{\ln T}\right)\left[\frac{\sigma(T)}{T}\right] \ . \tag{9-4}$$

This expression shows that there is a range of transmission values over which the relative precision of the density measurement is smaller than that of the transmission (the favorable precision regime, $|\ln T| > 1$ or $T < 0.37$. For larger transmission values, the relative precision of the density is larger than that of the transmission and the measurement suffers accordingly. Note that when T approaches 1, the expression for the relative precision diverges because of the factor $1/(\ln T)$. Because the sample material is absorbing none of the incident radiation, there is no assay signal.

The range of useful transmission values can also be related to a characteristic concentration, $\rho_c = 1/\mu x$. When $\ln T > 1$, then $\rho > \rho_c$ and the measurement is in the favorable precision regime; but when $\rho < \rho_c$, the assay signal is too small and the precision is unfavorable. By determining the favorable operating range from

the point of view of this characteristic concentration, one can choose a reasonable sample thickness (x), given the intrinsic properties of the sample material to be measured (μ) and the expected range of sample concentrations.

Because of the symmetry in ρ and x in Equations 9-1 through 9-3, Equation 9-4 also expresses the relative precision of a thickness measurement. For a thickness measurement, the precision can be enhanced by a judicious choice of photon energy.

There are limits both on how high and on how low the sample transmission should be for optimum measurement precision. Because $T = I/I_0$ and the intensities are statistically varying quantities, Equation 9-4 can be rewritten as

$$\frac{\sigma(\rho)}{\rho} = \frac{1}{\ln T}\left(\frac{T+1}{I_0\,T}\right)^{1/2} \qquad (9\text{-}5)$$

A plot of this relationship in Figure 9.2 shows the deterioration of the measurement precision at the high- and low-concentration extremes. The optimum range of T is below the point where $\ln T = 1$, in keeping with the definition of ρ_c. The range of T over which the quantity $\sigma(\rho)/\rho$ is near a minimum determines the instrument design features (sample thickness, measurable concentration range, and photon energy). These features are also important in the more complex densitometry measurements described in Sections 9.3 and 9.4.

Note that the above discussion deals with the measurement precision determined by counting statistics alone. Generally, other factors can cause added fluctuations in the measurement results; they include variations in the matrix material (solvent) and possible instrumental fluctuations. As a result, the precision of an assay instrument should be determined by making replicate measurements of known standards representing the full range of sample and solvent properties.

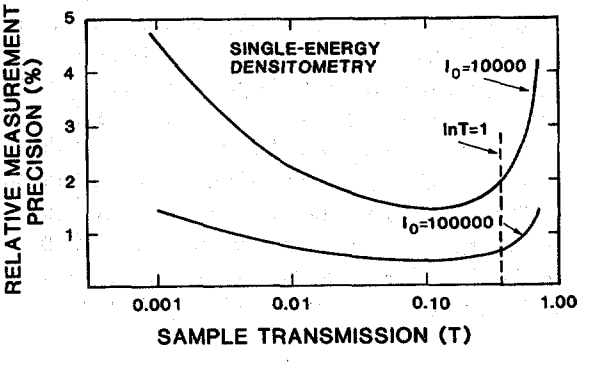

Fig. 9.2 *Precision of single-energy densitometry as a function of sample transmission for two values of incident photon total counts (from Equation 9-5). The optimum transmission is that which gives the smallest relative measurement precision. This corresponds to a concentration that is greater than the characteristic concentration, ρ_c, where $\ln T = 1$. (Note the logarithmic scale on the horizontal axis.)*

9.3 MULTIPLE-ENERGY DENSITOMETRY

Measurement of photon transmission at one energy allows for the assay of only one substance or of only one component of a mixture; the concentration of the other components must be kept constant. Measurement of photon transmission at two energies allows for the assay of two components of a mixture. Such a compound measurement stands the greatest chance for success the more the attenuation coefficients of the two components differ from one another. Analysis of the concentration of a high-Z element in a low-Z solvent is an excellent example of a two-energy densitometry measurement.

9.3.1 Analysis of Two-Energy Case

Consider a mixture of two components with (unknown) concentrations ρ_1 and ρ_2. Let the mass attenuation coefficient of component i measured at energy j be given by

$$\mu_i^j = \mu_i(E_j) \tag{9-6}$$

and define the transmission at energy j as

$$T_j = \exp\left[-\left(\mu_1^j\rho_1 + \mu_2^j\rho_2\right)x\right] . \tag{9-7}$$

The measurement of two transmissions gives two equations for the two unknown concentrations:

$$\begin{aligned}(-\ln T_1)/x = M_1 &= \mu_1^1\rho_1 + \mu_2^1\rho_2 \\ (-\ln T_2)/x = M_2 &= \mu_1^2\rho_1 + \mu_2^2\rho_2 .\end{aligned} \tag{9-8}$$

By attributing the measured absorption to the two sample components, we are actually defining the incident radiation to be the intensity transmitted by an empty sample container. The solution to the above equations is

$$\begin{aligned}\rho_1 &= (M_1\mu_2^2 - M_2\mu_2^1)/D \\ \rho_2 &= (M_2\mu_1^1 - M_1\mu_1^2)/D \\ D &= \mu_1^1\mu_2^2 - \mu_2^1\mu_1^2 .\end{aligned} \tag{9-9}$$

For Equation 9-8 to have a solution, the determinant of the coefficients, D, must be nonzero. This condition is virtually assured if the mass attenuation coefficients for the two components have significantly different energy dependences. Physically, this has the meaning that the assay is feasible if the components can be distinguished from one another by their absorption properties. This criterion further suggests two possible choices of photon energies. First, if two widely differing energies are used, the differ-

ent slopes of μ vs E for the high-Z and the low-Z components suffice to differentiate between them. Second, by choosing photon energies near and on either side of an absorption edge for the heavier (higher-Z) component, the energy dependence for the mass attenuation coefficient of the higher-Z material will appear to have the opposite slope to that of the low-Z component, making the two components easily distinguishable. This approach is especially promising in assays of SNM in low-density matrices or in assays of two SNM components.

9.3.2 Measurement Precision

The primary source of random measurement uncertainty is the statistical variance of the transmission measurements. The expression for the relative precision of each component's concentration is given by

$$\frac{\sigma(\rho_1)}{\rho_1} = \frac{1}{\mu_2^1 \ln T_2 - \mu_2^2 \ln T_1} \left\{ \left[\mu_2^2 \frac{\sigma(T_1)}{T_1}\right]^2 + \left[\mu_2^1 \frac{\sigma(T_2)}{T_2}\right]^2 \right\}^{1/2}$$

$$\frac{\sigma(\rho_2)}{\rho_2} = \frac{1}{\mu_1^2 \ln T_1 - \mu_1^1 \ln T_2} \left\{ \left[\mu_1^2 \frac{\sigma(T_1)}{T_1}\right]^2 + \left[\mu_1^1 \frac{\sigma(T_2)}{T_2}\right]^2 \right\}^{1/2} \quad (9\text{-}10)$$

Note that because the assay result varies inversely with the sample thickness (see Equation 9-8), the sample thickness (x) must be very well known or held constant within close tolerance.

9.3.3 Extension to More Energies

In principle, the multiple-energy densitometry technique can be extended to three or more energies to measure three or more sample components. In practice, such a broadening of the technique undermines the sensitivity of the measurement for some sample components, because it is extremely difficult to select gamma-ray energies that can sample different energy dependences of the absorption of each of the components. Accordingly, multiple-energy densitometry is rarely extended beyond the two-energy case.

9.4 ABSORPTION-EDGE DENSITOMETRY

Absorption-edge densitometry is a special application of two-energy densitometry. The photon energies at which the transmissions are measured are selected to be as near as possible to, and on opposite sides of, the absorption-edge discontinuity in the energy dependence of the mass attenuation coefficient for the unknown material (Ref. 1). Both the K and the L_{III} absorption edges have been used in nondestructive

assay of special nuclear material (see Section 9.7 for specific applications). Figure 9.3 shows the attenuation coefficients for plutonium, uranium, and selected low-Z materials and includes the K and L edges for the heavy elements.

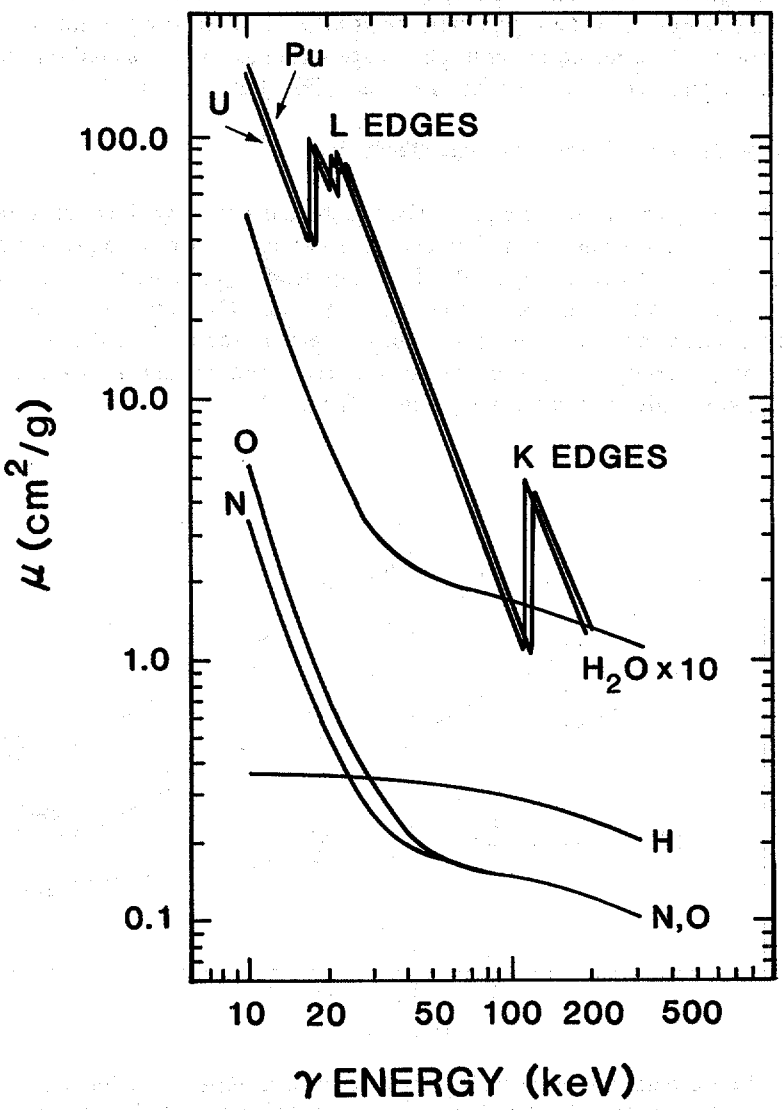

Fig. 9.3 *Energy dependence of the photon mass attenuation coefficients for uranium, plutonium, and selected low-Z materials. Note the absorption-edge discontinuities for uranium and plutonium in the 17- to 20-keV (L edge) and 115- to 122-keV (K edge) energy regions.*

Absorption-edge densitometry involves the measurement of the transmission of a tightly collimated photon beam through the sample material. The collimation defines the measurement geometry and also reduces interference from radiation emitted by the sample material. Because the collimation selects only a small fraction of the sample volume, the sample must be highly uniform for the assay to be representative of all of the material. As a result, the absorption-edge technique is best suited for solution assays, although it has been used for assays of solids (Refs. 2 through 4).

9.4.1 Description of Measurement Technique

Consider the typical case of a high-Z (SNM) component in a low-Z (solvent) matrix. Figure 9.4 depicts the attenuation coefficients and measurement energies above (U) and below (L) an absorption edge. (The discussion emphasizes K-edge measurements, but the analysis is similar in the L-edge region as well.) The subscript s refers to the measured element, and the subscripts M and m refer to the high- and low-Z matrix elements, respectively. The magnitudes of the attenuation coefficient discontinuities and the edge energies of interest are given in Table 9-1.

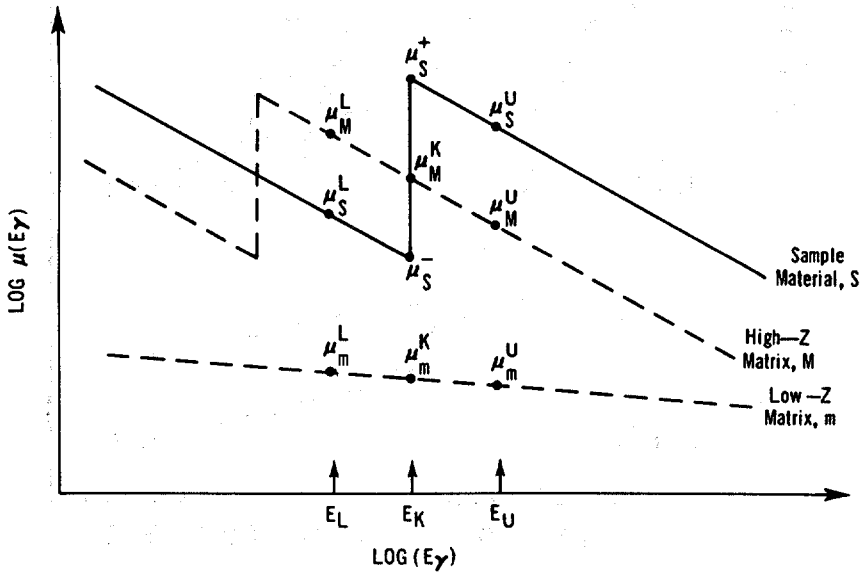

***Fig. 9.4** Expanded schematic of the mass attenuation coefficient as a function of photon energy. Curves are shown for a sample material (s), assumed to be a heavy element, a heavy-element matrix component (M), and a light-element matrix component (m).*

Table 9-1. Absorption-edge energies and discontinuities for selected SNM components

Property	Uranium	Plutonium
E(K)	115.6 keV	121.8 keV
$E(L_{III})$	17.2 keV	18.0 keV
$\Delta\mu$(K)	3.7 cm^2/g	3.4 cm^2/g
$\Delta\mu(L_{III})$	55.0 cm^2g	52.0 cm^2/g

Equation 9-11 gives the transmission of photons through the solution at the two measurement energies E_U and E_L.

$$\ln T_L = -(\mu_s^L \rho_s + \mu_m^L \rho_m)x$$
$$\ln T_U = -(\mu_s^U \rho_s + \mu_m^U \rho_m)x \; . \tag{9-11}$$

To solve for the measured element concentration,

$$\rho_s = \frac{1}{\Delta\mu x}\ln\left(\frac{T_L}{T_U}\right) + \rho_m\left(\frac{\Delta\mu_m}{\Delta\mu}\right) \tag{9-12}$$

where

$$\Delta\mu = \mu_s^U - \mu_s^L > 0$$
$$\Delta\mu_m = \mu_m^L - \mu_m^U > 0 \; . \tag{9-13}$$

The second term in Equation 9-12 expresses the contribution from the solvent matrix. Because the transmissions are measured relative to an empty sample container, the transmission of the sample container does not influence Equation 9-12. Note the similarity of Equation 9-12 to the single-line case (Equation 9-3), with μ's replaced by $\Delta\mu$'s.

Because the matrix term in Equation 9-12 is independent of SNM concentration and sample cell geometry, it can be applied to any absorption-edge densitometry measurement for which the solution transmissions are measured relative to an empty sample container. Ideally, if $E_L = E_U = E_K$, then $\Delta\mu_m = 0$, and the measurement is completely insensitive to any effects from the matrix. In practice, however, the two measurement energies differ by a finite amount, so some residual matrix correction may be necessary. In cases where the matrix contribution may be significant, it can be determined empirically by assaying a solution that contains only the matrix material or its effect can be deduced analytically. For further discussion of matrix corrections for absorption-edge densitometry, see Section 9.4.4.

The ratio of the two transmissions at the two measurement energies ($R = T_L/T_U$) is the measured quantity, and $\Delta\mu$ and x are constants that can be evaluated from

transmission measurements with calibrated standards of well-defined concentrations. With judiciously chosen photon energies, this technique will provide very reliable, nearly matrix-independent assays of specific elements whose absorption edges lie between the transmission source energies.

9.4.2 Measurement Precision

Differentiation of Equation 9-12 gives the relative precision of a densitometry measurement:

$$\frac{\sigma(\rho_s)}{\rho_s} = \left(\frac{1}{\Delta\mu\rho_s x}\right)\left[\frac{\sigma(R)}{R}\right] = \left(\frac{1}{\ln R}\right)\left[\frac{\sigma(R)}{R}\right] . \tag{9-14}$$

The fractional error in R is determined by the counting statistics of the transmission measurements. In analogy with the discussion of Equation 9-4, the choice of measurement parameters can be guided by reference to a characteristic concentration, $\rho_c = 1/\Delta\mu x$. When $\rho > \rho_c$, the measurement is in the favorable precision regime, where $\sigma(\rho)/\rho < \sigma(R)/R$. But if the SNM concentration is too far above ρ_c, the excessive absorption deteriorates the measurement precision, primarily because of the enhanced absorption of the transmission gamma rays above the absorption edge. The statistical fluctuations of the very small transmitted intensity at E_U is then overpowered by the statistical fluctuations of the background in that energy region.

Table 9-2 shows the values of these characteristic concentrations for a 1-cm transmission path length (x = 1 cm). The table implies, for example, that for a 1-cm sample cell thickness, K-edge assays of plutonium concentrations greater than 300 g/L would be in the favorable precision regime. For assays of 30-g/L solutions, the sample cell thickness should be greater than 0.5 cm for L_{III}-edge assays and greater than 9 cm for K-edge assays.

Table 9-2. Characteristic concentrations for uranium and plutonium

Characteristic Concentration	Uranium (g/L)	Plutonium (g/L)
ρ_c(K)	270	294
$\rho_c(L_{III})$	18	19

A more analytical approach can be used to optimize measurement parameters. Figure 9.5 shows the calculated statistical measurement precision (Equation 9-14) as a function of transmission path length (x) for a variety of SNM concentrations. The figure shows, for example, that a densitometer designed for 30-g/L SNM solution assays should have a sample cell thickness of 7 to 10 cm.

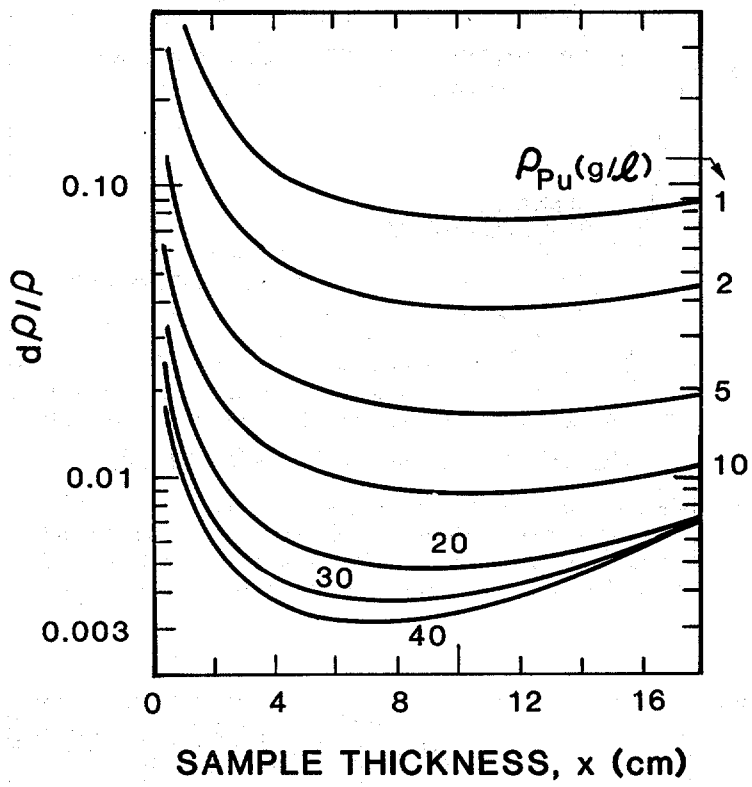

Fig. 9.5 Calculated relative statistical uncertainty in plutonium concentration by K-edge densitometry as a function of sample cell thickness (transmission path length). The empty cell transmission counts below the K edge (I_{0L}) were taken to be 2 × 10^6 in the 121.1-keV photopeak.

The final test in evaluating the design of a densitometer is empirical determination of the assay precision. Figure 9.6 shows the precision of a series of measurements on a K-edge densitometer designed for low- to medium-concentration plutonium solution assays with a 7-cm-thick sample cell (Ref. 5). Figure 9.6 agrees well with the theoretical curve shown in Figure 9.5.

Calculations of measurement precision are helpful in determining design parameters for optimum instrument performance. Figure 9.7 shows the results of such calculations for both K- and L_{III}-edge densitometers (Ref. 6). The ranges of plutonium concentrations over which the relative measurement precision is better than 1% are shown for different sample thicknesses (x).

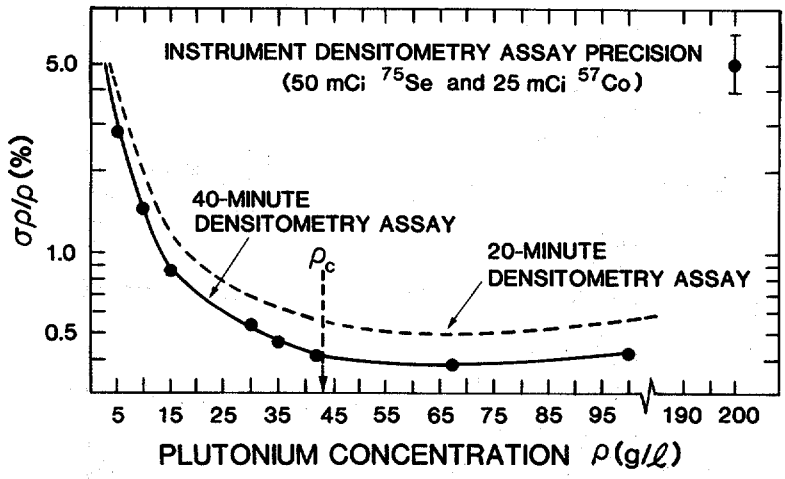

Fig. 9.6 Relative statistical precision achieved in a plutonium concentration measurement by K-edge densitometry as a function of sample concentration, for a sample cell thickness of 7 cm. Note the broken scale above 100 g/L. Curves are shown for two count times (Ref. 5).

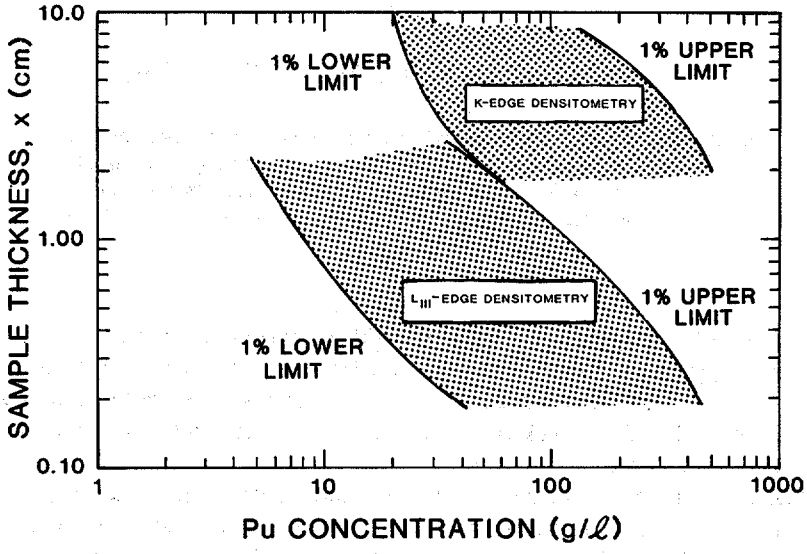

Fig. 9.7 Indications of sample transmission thicknesses (x) over which plutonium concentration assays can be performed by absorption-edge densitometry to better than 1% statistical precision. Shaded regions for the K- and L_{III}-edge techniques show plutonium concentration ranges over which this precision is achievable.

9.4.3 Measurement Sensitivity

A useful parameter in the specification of a nondestructive assay instrument is its "minimum detectable limit," which is that quantity of nuclear material that produces an assay signal significantly above background in a reasonable count time (Refs. 7 and 8). For nuclear waste measurements, where the minimum detectable limit is an important instrument specification, an assay signal that is three standard deviations (99% confidence level) (Ref. 9) above background is considered to be significant. This limit can also be regarded as a measurement sensitivity, in that it characterizes a lower limit of SNM that can be detected with some level of confidence.

Because absorption-edge densitometers are usually built for specific assay applications in well-defined SNM solution concentration ranges, the minimum detectable limit is not particularly important. However, the measurement sensitivity can serve as a convenient quantity for comparing design approaches and other factors that influence instrument performance.

To obtain an expression for the measurement sensitivity of an absorption-edge densitometer, the assay background must be defined so that the minimum detectable assay signal can be determined. The statistical uncertainty in the measured density is given in Equation 9-14. The ratio R of the two transmissions above and below the absorption edge is composed of raw gamma-ray (or x-ray) photon intensities that vary according to the usual statistical prescriptions. When the SNM concentration is zero, the solution is entirely matrix material (typically acid) and

$$T_U \approx T_L = T = \exp(-\mu_m \rho_m x) \; . \tag{9-15}$$

When the the SNM concentration is zero, R = 1. Then the definition of T gives

$$\sigma(\rho) = \frac{1}{\Delta\mu x}\left(\frac{1}{I_{0U}} + \frac{1}{I_{0L}} + \frac{1}{TI_{0U}} + \frac{1}{TI_{0L}}\right)^{1/2} \; . \tag{9-16}$$

Equation 9-16 expresses the uncertainty in the background. The three-sigma criterion provides an expression for the minimum detectable limit (or sensitivity, s) for an absorption-edge densitometer:

$$s = \frac{3}{\Delta\mu x}\left[\left(\frac{1}{I_{0U}} + \frac{1}{I_{0L}}\right)\left(\frac{T+1}{T}\right)\right]^{1/2} \quad (g/L) \tag{9-17}$$

where the units of $\Delta\mu x$ are cm^3/g.

Equation 9-17 shows that the measurement sensitivity is affected by several measurement parameters:

- The sensitivity suffers in low-transmission samples.
- Long counts of the unattenuated photon intensities (I_0) improve measurement sensitivity.

- L-edge measurements (with their larger $\Delta\mu$ are more sensitive than K-edge measurements (if all other measurement parameters remain the same).
- An increase in sample cell thickness may improve the measurement sensitivity, but the accompanying decrease in T will compete with that improvement.

9.4.4 Matrix Effects

The absorption-edge technique is insensitive to the effects of matrix materials if both transmissions are measured at the absorption edge. However, with a finite energy separation of the transmission gamma rays, the matrix contribution is nonzero and is represented by the second term in Equation 9-12. This term can become significant for low SNM concentrations, ρ_s, or when the spacing between the assay energies, E_L and E_U, becomes large; either condition threatens the validity of the inequality $\Delta\mu_m\rho_m \ll \Delta\mu\rho_s$.

The natural width of the absorption edge (less than 130 eV) and the energy resolution of the detection system (typically 500 eV or more) are intrinsic limitations to the design of an instrument that attempts to minimize the effects of matrix attenuation by using closely spaced assay energies. The limited availability of useful, naturally occurring radioisotopes also leads to compromises in the choice of transmission sources.

One very useful technique for reducing the matrix effect is an extrapolation procedure applied to the measured transmission data (Refs. 2 and 5). The procedure attempts to extrapolate the measured transmissions to the energy of the absorption edge. This extrapolation is possible because the energy dependence of the mass attenuation coefficients over narrow energy ranges is known to be a power law:

$$\log \mu(E) = k \log E + B \ . \tag{9-18}$$

The slope parameter (k) is essentially the same for elements with $Z > 50$, with an average value of approximately -2.55 near the uranium and plutonium K edges (Ref. 2). Table 9-3 gives the extracted values for the slopes and intercepts of several substances of interest to SNM assay (Ref. 10).

As an example of a general assay case, consider a solution of SNM in a low-Z solvent, with possible additional heavy-element ($Z > 50$) matrix contaminants. Equation 9-12 generalizes to

$$\rho_s = \left(\frac{1}{\Delta\mu x}\right)\ln\left(\frac{T_L}{T_U}\right) + \rho_M\left(\frac{\Delta\mu_M}{\Delta\mu}\right) + \rho_m\left(\frac{\Delta\mu_m}{\Delta\mu}\right) \ . \tag{9-19}$$

The subscript M refers to the high-Z matrix contaminant, and the subscript m represents the low-Z matrix (solvent); and in analogy with Equation 9-13, $\Delta\mu_M = \mu_M^L - \mu_M^U$ (see Figure 9.4). The measured transmissions are then extrapolated to the SNM K edge using the energy dependence of $\mu(E)$ for the heavy elements. Because the slope parameters (k) for $Z > 50$ are all essentially the same, the SNM and high-Z

Table 9-3. Slopes (k) and intercepts (B) for the linear dependence of log μ(E) vs log E for various materials of interest in the 100- to 150-keV energy region (log to base 10)[a]

Solution Component	k	B
Plutonium (above K edge)	−2.48	5.83
(below K edge)	−2.56	5.42
Uranium (above K edge)	−2.49	5.82
(below K edge)	−2.71	5.65
Tungsten	−2.50	5.65
Tin	−2.45	5.12
Iron	−1.57	2.70
Aluminum	−0.500	0.227
Water	−0.306	−0.153
Nitric Acid	−0.314	−0.171

[a]Ref. 10.

matrix absorption coefficients can be transformed with the same k (for example, the average value, −2.55). As a result, the transformed $\Delta\mu_M$ vanishes and the assay result becomes

$$\rho_s = \left(\frac{1}{\Delta\mu_{\pm}\mathrm{x}}\right)\ln\left(\frac{\mathrm{T}_L^a}{\mathrm{T}_U^b}\right) + \left(\frac{\mathrm{c}\mu_m^K\rho_m}{\Delta\mu_{\pm}}\right) \tag{9-20}$$

where $\Delta\mu_{\pm}$ (which equals $\mu_s^+ - \mu_s^-$, see Figure 9.4) is now defined across the absorption edge (in this case, the K edge) rather than between the energies E_L and E_U. The constants a, b, and c are defined as

$$\begin{aligned} \mathrm{a} &= (\mathrm{E}_K/\mathrm{E}_L)^k \\ \mathrm{b} &= (\mathrm{E}_K/\mathrm{E}_U)^k \\ \mathrm{c} &= (\mathrm{E}_K/\mathrm{E}_L)^{k-k'} - (\mathrm{E}_K/\mathrm{E}_U)^{k-k'} \end{aligned} \tag{9-21}$$

where k = −2.55 and k′ = −0.33 (the average value of k for elements with atomic numbers less than 10). This procedure renders the assay essentially independent of the heavy-element matrix but still leaves a residual correction for the light-element matrix. It is not possible to remove the effects of both the light- and heavy-element matrix materials because $k \neq k'$. The transmissions must be corrected for the acid matrix contributions because the transmissions are measured relative to an empty sample cell. If the reference spectra (the I_0 intensities) were taken with the cell full of a representative acid solution, no acid matrix correction would be necessary. However,

any fluctuation in acid molarity would bias the measurement of an actual sample. The density of nitric acid (ρ_m) and the acid molarity (M) are related (Ref. 11) by

$$\rho_m = 1 + 0.03\ \mathrm{M}\ . \tag{9-22}$$

For plutonium K-edge assays in which the K edge is closely bracketed by ^{57}Co and ^{75}Se gamma rays (see Section 9.4.6), this low-Z matrix correction is small but may be important at low plutonium concentrations. For example, the correction term in Equation 9-20 for 3 M nitric acid is equivalent to approximately 0.87 g Pu/L (Ref. 5). Equation 9-22 shows that fluctuations in acid molarity cause fluctuations in the acid matrix correction that are only 3% as large; so careful control of the acid molarity is important only at very low SNM concentrations.

For uranium K-edge assays with a ^{169}Yb transmission source (E_L = 109.8 keV, E_U = 130.5 keV), the extrapolation procedure greatly improves the quality of the assay results. This is demonstrated graphically in Ref. 2, where assays of uranium solutions with varying tin concentrations were shown to be matrix-independent with the extrapolation correction. Several other matrix effects studies are described in Ref. 12.

9.4.5 Choice of Measurement Technique

Because of differences in the $\Delta\mu$ values at the K edge versus the L_{III} edge, the measurement sensitivity (defined in Equation 9-17) is more than an order of magnitude larger at the L_{III} edge than at the K edge, other parameters being equal (see also Table 9-1). However, because of the higher penetrability of photons at the K-edge energies, thicker samples can be used for the K-edge measurements, thereby enhancing K-edge sensitivity.

If significant quantities of lower-Z elements (such as yttrium and zirconium) are present in a sample, the K edges of these elements cause discrete interferences that bias the L_{III} assays of uranium and plutonium (Ref. 12). Furthermore, detector resolution at L_{III} energies limits the ability to perform L_{III}-edge assays in the presence of significant amounts of neighboring elements (uranium with protactinium or neptunium; plutonium with neptunium or americium). The K-edge measurements are not subject to such interferences. In addition, the higher photon energies required for the K-edge transmission measurements permit the use of thicker or higher-Z materials for sample-cell windows, an important practical consideration for in-plant operation. Finally, more flexibility exists in the availability of discrete-gamma-ray transmission sources for K-edge measurements.

9.4.6 Transmission Sources

The most versatile transmission source is the bremsstrahlung continuum produced by an x-ray generator. The intensity of this source can be varied to optimize the count rate for a variety of sample geometries, concentrations, and thicknesses.

The x-ray generator voltage (which determines the assay energy range) can be adjusted and the spectrum tailored appropriately for the assay of specific elements. Furthermore, matrix effects can be minimized by extrapolation of the measured transmissions to the absorption edge. Commercial units are available with power supplies that are highly stable and x-ray tubes that are long-lived for long-term reliable operation in either the K- or the L_{III}-edge energy regions.

The use of discrete gamma-ray lines that bracket the absorption edge, the alternative to the continuum transmission sources, has been demonstrated successfully in several instruments. This technique is appropriate for K-edge assays. Discrete gamma rays are not available as primary emissions in the L_{III}-edge energy region. This approach depends on the availability of relatively slowly decaying radioisotopes that emit gamma rays of appropriate energies and sufficient intensities. For example, a convenient combination for the K-edge assay of plutonium (E_K = 121.8 keV) is the 121.1-keV gamma ray from ^{75}Se (half-life = 120 days) and the 122.1-keV gamma ray from ^{57}Co (half-life = 270 days). The proximity of both energies to the plutonium absorption edge minimizes the effects of the matrix and enhances the sensitivity of the assay (Ref. 1). Because of the different half-lives, accurate decay corrections or frequent measurements of the unattenuated intensities (I_0) are required. The use of ^{169}Yb (half-life = 32 days) for uranium assay at the K edge (Refs. 2 and 3) has the advantage of requiring no decay correction because both gamma rays come from the same source. However, the larger energy separation (E_L = 109.8 keV, E_K = 115.6 keV, E_U = 130.5 keV) introduces a larger matrix sensitivity (larger $\Delta\mu_m$) and a smaller assay sensitivity (smaller $\Delta\mu$). Furthermore, to maintain acceptable counting statistics, the source must be replaced frequently because of the short half-life of ^{169}Yb. The extrapolation technique discussed in Section 9.4.4 is especially effective in reducing the matrix sensitivity. A detailed discussion of convenient radioisotopic sources for absorption-edge densitometry appears in Ref. 1. Several variations on these two basic transmission source configurations are discussed in Ref. 12.

9.5 SINGLE-LINE DENSITOMETERS

The measurement of photon transmission at a single energy has been applied using low-resolution detectors for assay of SNM in solution and in reactor fuel elements. These instruments use low-energy gamma-ray transmission sources to minimize the ratio μ_0/μ (see Equation 9-3) and thus reduce the sensitivity to variations in the low-Z matrix.

One instrument uses an ^{241}Am transmission source mounted in the center of an annular cell containing SNM solution (Refs. 13 and 14). The cell is surrounded by a 4π plastic scintillator. The instrument separates the transmitted 60-keV gamma ray from the background sample radiation by modulating the source with a rotating, slotted tungsten shield. Designed to assay high concentrations (>200 g/L) of SNM, the instrument is sensitive to 1% changes in SNM concentration at the 95% confidence level.

A single-line densitometer has been used to determine the density of SNM in pelleted and compacted ceramic fuel elements (Ref. 15). The 67- and 76-keV gamma rays of ^{171}Tm and the 84-keV gamma ray of ^{170}Tm are detected by a 1-in.-diam NaI(Tl) detector. The gross detector signals are counted in the multichannel scaling mode as the fuel elements are scanned to give the SNM density profile. The sensitivity of the instrument to SNM is 0.2 g/cm^3 at the 95% confidence level.

9.6 DUAL-LINE DENSITOMETERS

Dual-line densitometry has application to solids (fuel elements) and to solutions. Low- and high-resolution gamma spectrometers have been used and have been applied to the assay of a low- and high-Z component, as well as to the assay of two high-Z components.

A dual-line densitometer has been used to determine the densities of the low-Z (silicon and carbon) and high-Z (thorium and uranium) components in high-temperature gas-cooled reactor (HTGR) fuel pellets (Refs. 16 and 17). The transmission source provides two widely differing gamma-ray energies (122 keV from ^{57}Co and 1173 and 1332 keV from ^{60}Co), so that the sensitivity to the two components is based on the different slopes of μ vs E at low and high Z's. Equation 9-9 applies in this case. Fuel pellet cakes containing 92 to 95% thorium and 5 to 8% ^{238}U with a low-Z to heavy-Z weight ratio of 1.6 to 2.4 were assayed in 2-min measurement periods. The sensitivity to changes in the weight of either component was 3% or better at the 95% confidence level.

Dual-line solution densitometry has also been applied to the assay of two SNM components by measuring transmissions at two low gamma-ray energies (Refs. 18 and 19). The transmission energies were chosen to bracket the L-absorption edges of the higher-Z component (element 2) in such a way that, in Equation 9-8, $\mu_2^1 = \mu_2^2$ and $\mu_1^1 > \mu_1^2$. Thus, Equation 9-8 can be solved to give the concentration of element 1, independent of element 2:

$$\rho_1 = \left(\frac{1}{\Delta\mu_1 x}\right)\ln\left(\frac{T_1}{T_2}\right) \tag{9-23}$$

where $\Delta\mu_1 = \mu_1^2 - \mu_1^1$. The measured T_2 and ρ_1 are then used to obtain the concentration of element 2:

$$\rho_2 = \left(\frac{\ln T_2}{\mu_2^2}\right) - \frac{\rho_1\mu_1^2}{\mu_2^2} \tag{9-24}$$

Dual-line densitometry has been applied to thorium and uranium assay using secondary sources of niobium and iodine K_α x rays (at 16.6 and 28.5 keV, respectively) fluoresced by a 100-mCi ^{241}Am source. These x-rays bracket the L edges of uranium.

However, 16.6 keV is just above the L_{III} absorption edge of thorium (at 16.3 keV). Measurements were performed using low-resolution (Ref. 18) and high-resolution (Ref. 19) gamma-ray spectroscopy. The high-resolution experiments used reference solutions containing mixtures of thorium and uranium with total SNM concentrations between 35 and 70 g/L. In the range $0.25 \leq \rho_{Th}/\rho_U \leq 4.0$, the precision of the thorium and uranium concentration assay was 1% or better for 4000-s count periods.

9.7 ABSORPTION-EDGE DENSITOMETERS

Assay of uranium and plutonium solutions by the absorption-edge densitometry technique has been demonstrated in field tests of several instruments that perform K-edge or L_{III}-edge measurements. The instruments were designed for solution scrap recovery or reprocessing applications. Each instrument uses a high-resolution gamma-ray spectrometer (typically HPGe for K-edge assays and Si(Li) for L_{III}-edge assays) and a computer-based multichannel analyzer. The measurement precision achieved in each case approaches the statistical prediction, which is typically 0.5% or better for short ($\leq$30-min) count periods.

The transmission sources used by the K-edge instruments are discrete gamma-ray sources or bremsstrahlung continuum (x-ray) sources. The 109.8- and 130.5-keV gamma rays of ^{169}Yb are used for discrete K-edge assays of uranium, and the 121.1- and 122.1-keV gamma rays of ^{75}Se and ^{57}Co are used for discrete K-edge assays of plutonium. Only x-ray generators have been used in the L_{III}-edge instruments.

The absorption-edge assay relies on Equation 9-12. The assay precision (Equation 9-14) depends on several variables, including $\Delta\mu$, x, solution concentration, count time, and incident beam intensity. It is therefore convenient in comparing various instruments to use the characteristic concentration parameter $[\rho_c = (1/\Delta\mu x)]$ for each instrument. The instrument relative precision is defined as the precision measured at the optimum concentration for a fixed count period. This optimum concentration is that for which the relative precision $[\sigma(\rho)/\rho]$ is a minimum (see Figures 9.5 and 9.6).

Tables 9-4 and 9-5 list the K-edge and L_{III}-edge densitometers that have undergone field testing. The characteristic concentration (ρ_c) and the empirically determined optimum concentration (shown in parentheses beneath ρ_c) are given for each instrument. The tables specify the solutions used to obtain the data and quote the measured precisions at the optimum concentrations in specified count periods. Detailed discussions of the instruments listed in Tables 9-4 and 9-5 are given in Sections 9.7.1 and 9.7.2.

9.7.1 K-Absorption-Edge Densitometers

Given below are descriptions of several K-edge densitometers that have been tested and evaluated under actual or simulated in-plant environments. Table 9-4 summarizes the performance data for the instruments.

Table 9-4. K-absorption-edge densitometers.

Instrument Test Location	ρ_c ρoptimum (g/L)	SNM	Solution Type	Precision 1σ (%)	Live Time (s)	References
1. Los Alamos	135 (300)	U	HEU SR[a], misc.	0.5	1000	12,20,21
2. Oak Ridge Y-12	55 (100)	U	HEU SR, misc.	0.5	600	22,23
3. Barnwell AGNS	80 (200)	Pu	prepared (fresh, aged)	0.2	1200	12,24,25
4. Tokai (Japan) PNC	150 (300)	Pu	RP[b] product (fresh, aged)	0.2	2000	12,26,27,28
5. Savannah River SRP	40 (60)	Pu	RP product (fresh)	0.2	2000	5,12,29
6. Seibersdorf (Austria) IAEA (portable)	150 (300)	Pu	prepared	0.3	500	30
7. Karlsruhe (FRG) KfK (continuum source)	150 (300)	U	prepared	0.2	1000	12,31,32
		Pu	RP product	0.2	1000	
		U(+Pu)	[RP feed	0.2	1000	33
		Pu(+U)	U:Pu::3:1]	1.0	1000	

[a]SR = Scrap Recovery.
[b]RP = Reprocessing Plant.

Table 9-5. L_{III}-absorption-edge densitometers.

Instrument Test Location	ρ_c $\rho_{optimum}$ (g/L)	SNM	Solution Type	Precision 1σ (%)	Live Time (s)	References
1. Savannah River	16	U or Pu	RP[a] product	0.3	1000	12,21,34
SRL	(50)	U (+Pu)	[RP product	0.2	2000	
		Pu (+U)	U:Pu::2:1]	1.0	2000	
2. Argonne	16	U or Pu	prepared	0.3	1000	35
NBL	(50)	U (+Pu)	[prepared	0.2	2000	
		Pu (+U)	U:Pu::2:1]	0.9	2000	
3. Barnwell	19	U	U, natural	0.7	250	36
AGNS	(55)		enrichment (flowing)			
4. Los Alamos	16	U	U, natural	0.2	1000	37
(Compact)	(60)		enrichment			

[a]RP = Reprocessing Plant.

1. Los Alamos National Laboratory (Refs. 12, 20, and 21). The Los Alamos uranium solution assay system (USAS) is a hybrid assay instrument used off-line at the Los Alamos high-enriched uranium (HEU) scrap recovery facility. The USAS measurement head is shown in Figures 9.8 and 9.9.

The USAS applies three distinct gamma-ray methods to assay uranium concentration in 20- or 50-mL uranium solution samples (in disposable plastic sample vials) in three concentration ranges. Waste solutions with uranium concentrations in the range 0.001 to 0.5 g/L are counted for 2000 s with no transmission correction. Process solutions with concentrations in the range 1 to 50 g/L are measured using a ^{169}Yb transmission source. The highest range, 50 to 400 g/L, corresponding to product solutions, is assayed by the K-edge method using a ^{169}Yb transmission source. Accuracies of 0.7-1.5% can be achieved in measurement times of 400-2000 s.

The assay results are used for process control and nuclear material accounting. The instrument was in routine use in the scrap recovery facility from January 1976 until August 1984 when the facility was closed.

2. Oak Ridge Y-12 Plant (Refs. 22 and 23). The HEU scrap recovery facility at the Oak Ridge Y-12 Plant uses a solution assay system (SAS) that is analogous to the USAS. The K-edge method is used to assay 50-mL uranium solution samples in the concentration range 50 to 200 g/L. The samples include but are not limited to the product. The SAS uses a ^{169}Yb transmission source and disposable plastic sample vials.

Fig. 9.8 The USAS measurement head.

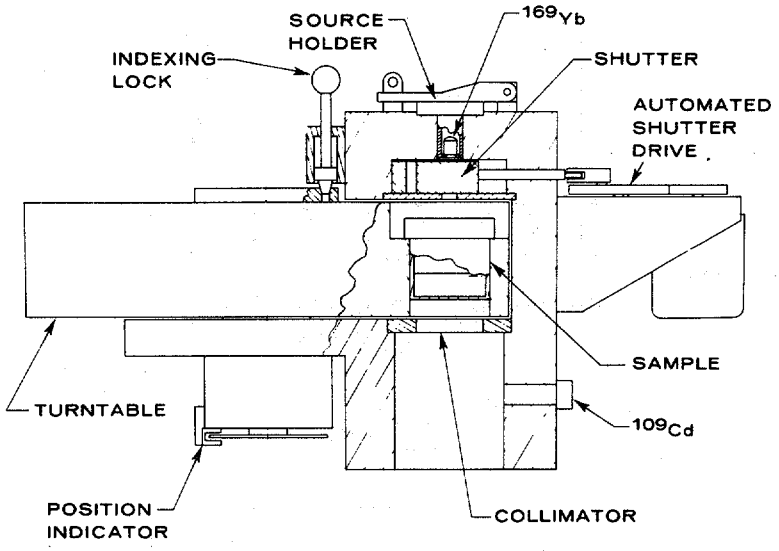

Fig. 9.9 *Scale line drawing of the USAS measurement head. The solution thickness in the transmission path is 2 cm.*

The system was put into routine use at Y-12 in October 1981 for process control and materials accounting.

3. Allied General Nuclear Services (AGNS) (Refs. 12, 24, and 25). A discrete-source K-edge densitometer was evaluated for plutonium assay at the Allied General Nuclear Services facility in Barnwell, South Carolina, during 1977-78. The hybrid instrument performed passive and K-edge measurements on prepared 10-mL solution samples of typical light-water-reactor plutonium in a fixed quartz sample cell. The transmission source was a combination of ^{75}Se and ^{57}Co. The results were reported for cells of different transmission path lengths.

4. Power Reactor and Nuclear Fuel Development Corporation (PNC) (Refs. 12 and 26 through 28). A discrete-source K-edge densitometer operates in the Tokai-Mura Reprocessing Plant analytical laboratory of the Power Reactor and Nuclear Fuel Development Corporation in Japan. Freshly separated and aged plutonium solution samples of the products of boiling-water-reactor and pressurized-water-reactor fuel reprocessing are assayed by the K-edge method in a two-cycle assay (first with a ^{75}Se transmission source, then with ^{57}Co). Figure 9.10 shows the location of the measurement station under the glove box at the Tokai-Mura plant laboratory. Figure 9.11 is a scale line drawing of the measurement head, which includes a well extending down from the glove-box floor. The instrument performs an isotopics assay on the fresh solutions in a third cycle. The solution samples are assayed in a well that is an

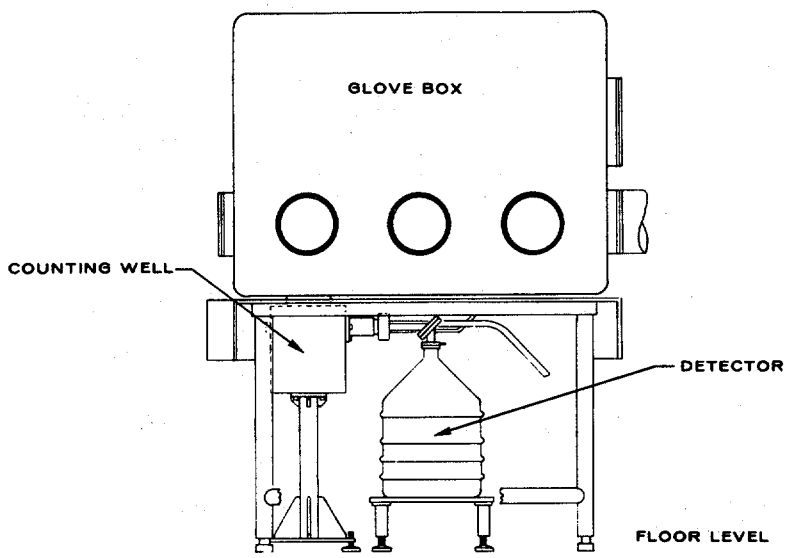

Fig. 9.10 *The Tokai K-edge densitometer measurement station beneath the laboratory glove box.*

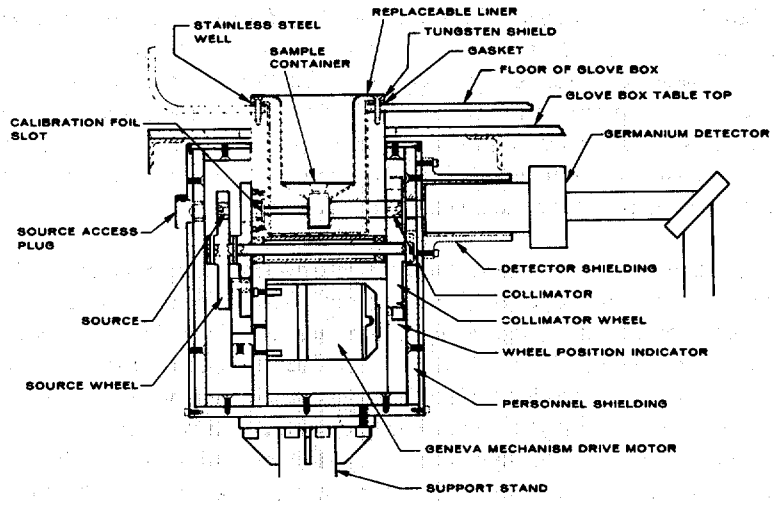

Fig. 9.11 *Scale line drawing of the Tokai K-edge densitometer measurement head. The solution thickness in the transmission path is 2 cm.*

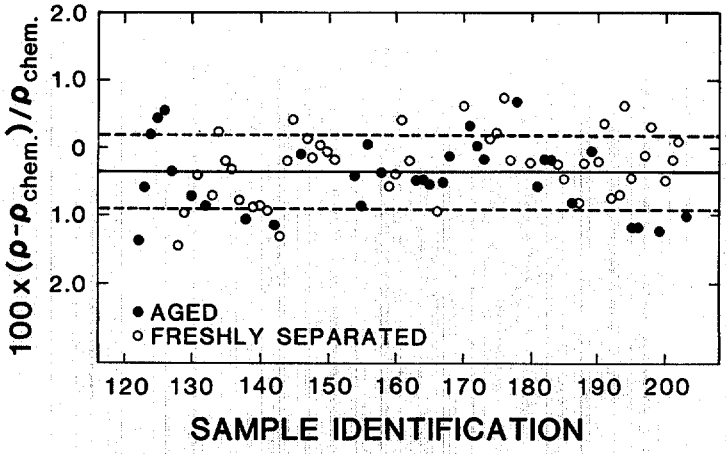

Fig. 9.12 *Percent difference between 600-s K-edge and destructive assays for plutonium concentration, plotted as a function of sample identification number. The solid line is the average relative result of −0.36%. This apparent bias is the result of calibration (in 1979) using only a small number of reference samples (see Ref. 27).*

extension of a glove box. The gamma-ray detector and the transmission sources are external to the glove box. The sample cells are disposable plastic vials that require approximately 10 mL of solution.

The Tokai instrument was installed in November 1979 and was operated through 1980 in an evaluation mode. The instrument has been in routine use in the facility since early 1981. Figure 9.12 is a plot of the percent difference between K-edge assay results and the reference values (from destructive analysis) obtained throughout 1981 during routine facility use of the instrument (Ref. 28). The densitometer has been available for facility use by IAEA inspectors since 1982.

5. Savannah River Plant (SRP) (Refs. 5, 12, and 29). A discrete-source K-edge plutonium solution densitometer was designed for in-line testing at the Savannah River Plant. A flow-through stainless steel sample cell was plumbed into a bypass loop on process solution storage tanks and resided in a protrusion of the process containment cabinet. The detector and transmission sources were located outside the containment cabinet on either side of the protrusion for measurement of the gamma-ray transmissions through the solution-filled cell. Figure 9.13 is a detailed illustration of the measurement station for this densitometer. Figure 9.14 illustrates the installation of the instrument in the process plumbing. The measurements were performed on

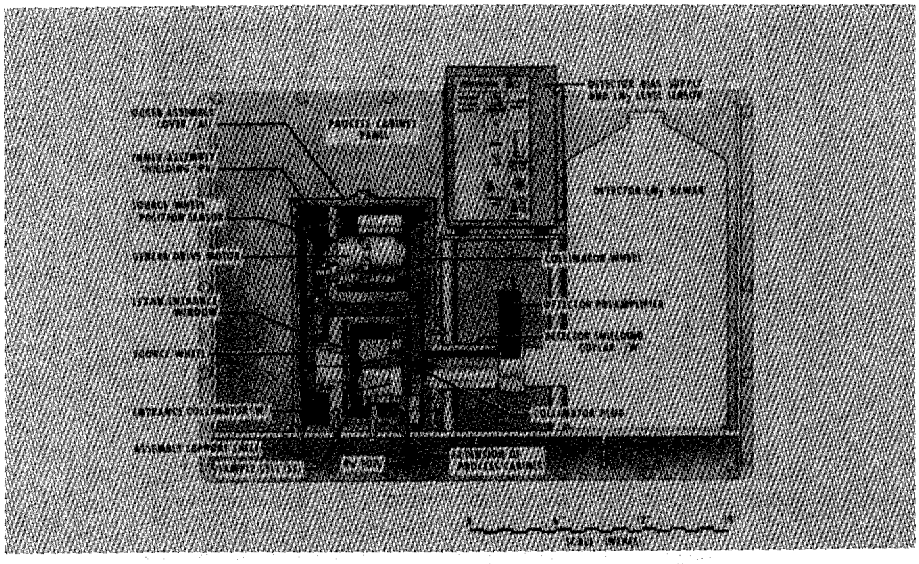

Fig. 9.13 *The measurement station for the SRP in-line plutonium solution densitometer. The source positioning mechanism and collimator wheels (shown at the left) straddle the process cabinet extension so that the sample cell (inside the process cabinet containment) is between the transmission sources and the detector, in a standard transmission-measurement geometry. The sample cell thickness is 7 cm.*

approximately 100 mL of static solution, after circulation of the tank solution through the bypass loop. (The freshly separated plutonium in the solutions is produced during reprocessing of low-burnup fuel.) The K-edge transmission measurements were performed in two cycles, as with the Tokai instrument, and a third cycle determined the plutonium isotopic composition. The instrument was also used to investigate the measurement of plutonium concentration in the presence of uranium admixtures. The extrapolation procedure described in Section 9.4.4 was used on solutions with uranium-to-plutonium ratios greater than 2:1 (see Ref. 5). The off-line testing of the instrument took place at the plant from April 1980 until December 1981. Figure 9.6 (see Section 9.4.2) is a plot of the measurement precision versus concentration (over the range 5 to 200 g/L) obtained in this testing phase (Ref. 5). The in-line testing began in December 1982 and ended in June 1983.

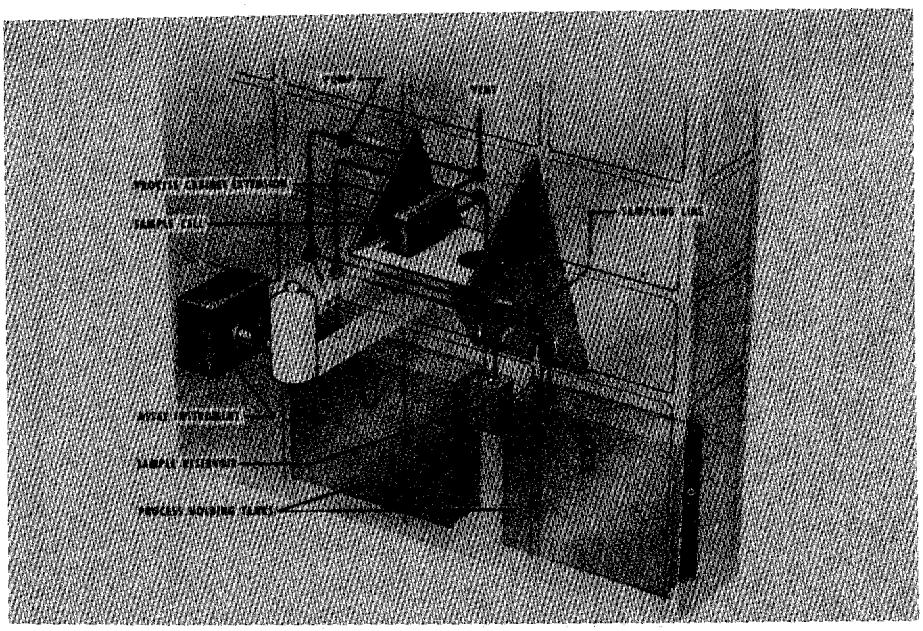

Fig. 9.14 In-line installation of the SRP plutonium solution densitometer. A by-pass plumbing loop brings plutonium-bearing solution from one of the holding tanks to the measurement cell. Provision is made for draining the cell into an intermediate reservoir so that samples of material just assayed can be removed for off-line verification by destructive analysis.

6. International Atomic Energy Agency (IAEA) Safeguards Analytical Laboratory (Ref. 30). A portable K-edge densitometer has been designed for testing as an inspection tool to authenticate the concentrations of plutonium samples inside glove boxes. The densitometer consists of hardware to hold and shield the detector and transmission sources and a portable multichannel analyzer equipped with electronics for the analog signal processing. The hardware slides inside the glove of the glove box so that a plutonium solution sample in a disposable plastic vial can be mounted and clamped in a holder between the detector and transmission source for the two-cycle K-edge assay. Figures 9.15 and 9.16 show the measurement head of the portable K-edge instrument inserted in a glove-box glove.

The portable densitometer has been tested at the IAEA's Safeguards Analytical Laboratory in Seibersdorf, Austria, since November 1983. A second unit is scheduled for field testing by IAEA inspectors in Japan.

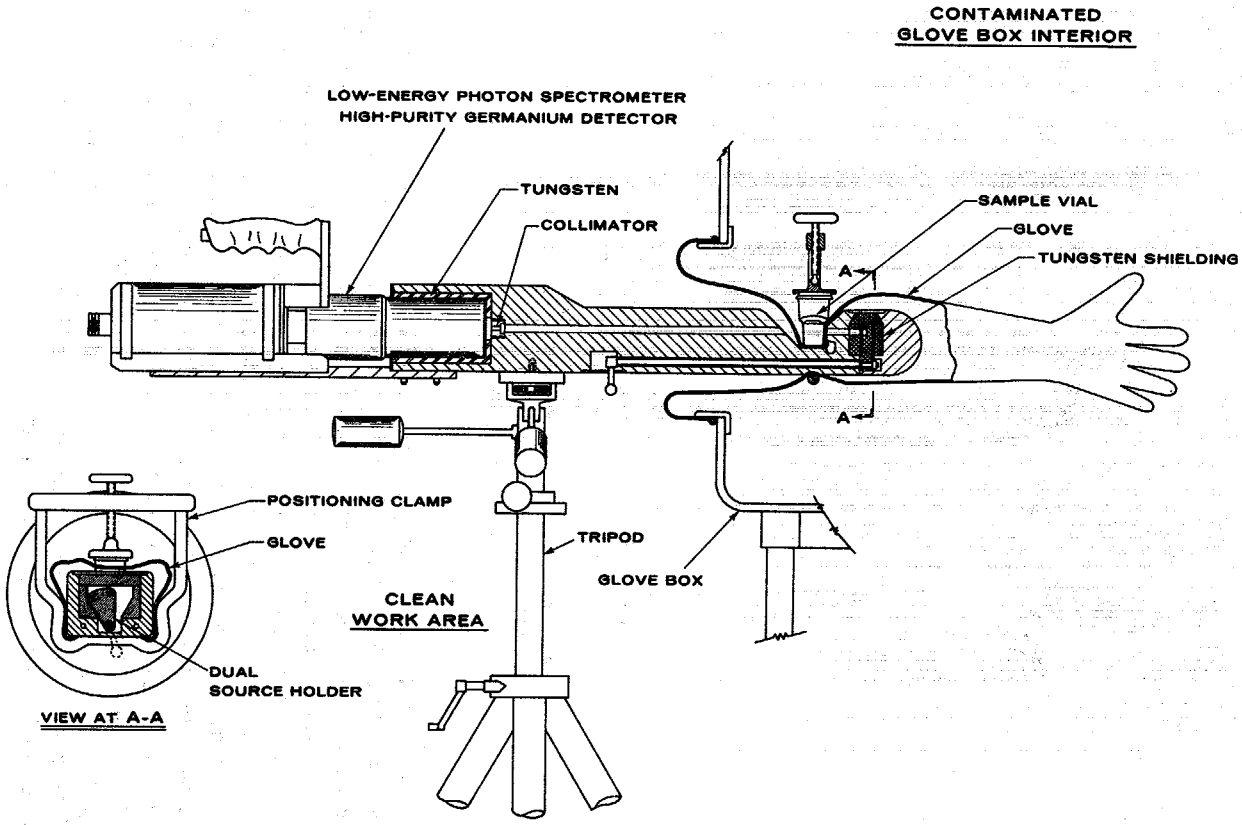

Fig. 9.15 Scale line drawing of the measurement head of the portable K-edge densitometer inserted in a glove-box glove. The sample cell thickness in the transmission path is 2 cm.

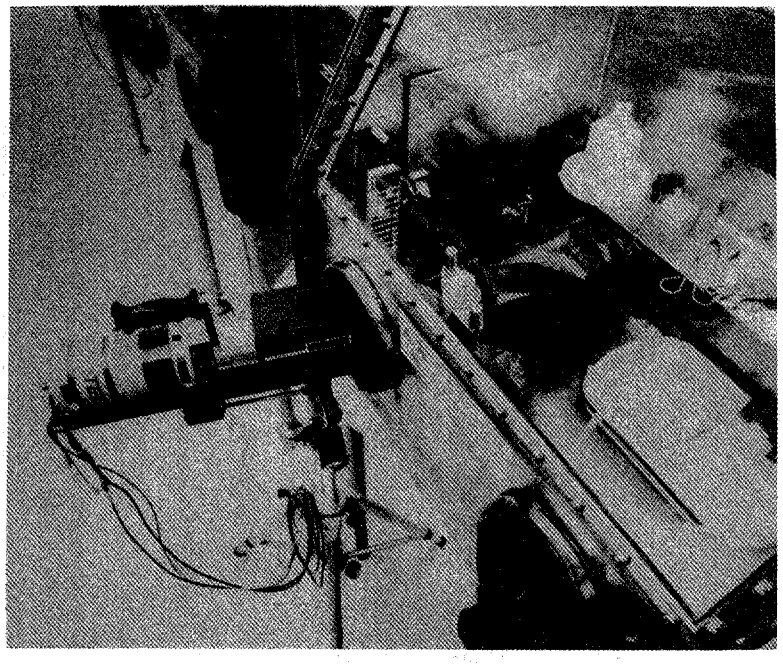

***Fig. 9.16** The portable K-edge densitometer, positioned for measurement.*

7. Kernforschungszentrum Karlsruhe (KfK) (Refs. 12 and 31 through 33). A continuum-source K-edge densitometer has been tested at Kernforschungszentrum Karlsruhe in Karlsruhe, Federal Republic of Germany (FRG), since 1978. The detector and x-ray head reside outside a glove box, and the samples and collimators are inside the glove box. The instrument has been used to assay reprocessing product solutions and fast-breeder-reactor reprocessing feed solutions for concentrations of both uranium and plutonium. A hybrid version of this instrument was used for assaying light-water-reactor feed solutions in which the plutonium content is approximately 1% of the uranium content. The continuum source served both as a transmission source for K-edge assay of uranium and as a fluorescing source for x-ray fluorescence (XRF) assay of the plutonium/uranium concentration ratio. The intensity of the continuum source allows the highly restrictive sample collimation required for K-edge and XRF assays while greatly reducing the passive count rate from the samples, which contain high levels of fission products.

Figure 9.17 is a line drawing of the measurement head for the hybrid instrument. Figure 9.18 shows the K-edge densitometer at Karlsruhe.

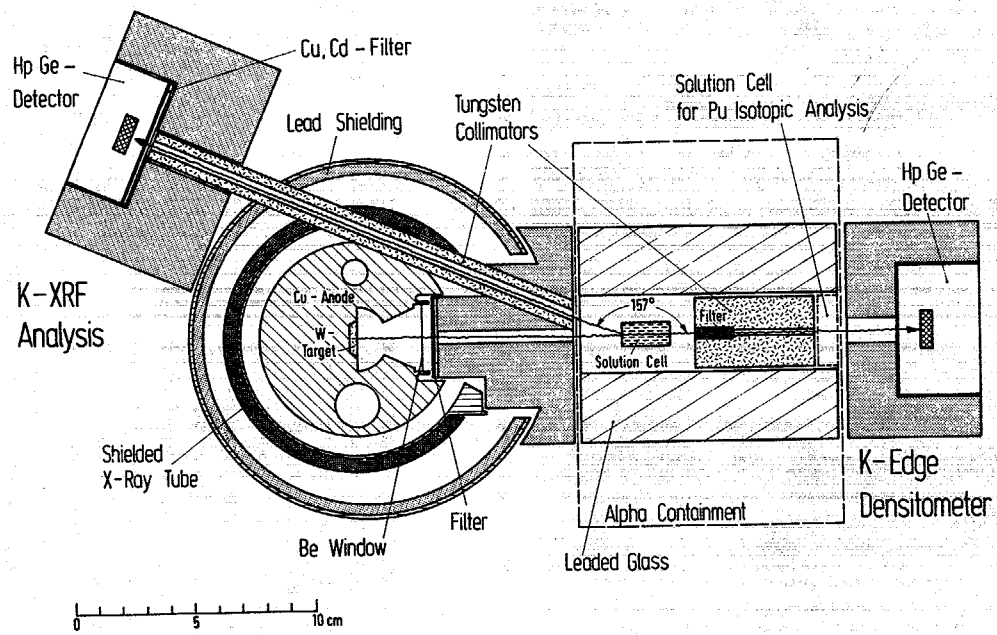

Fig. 9.17 *Cross-sectional view of the KfK combined K-edge/XRF system. The size of the alpha containment, a standard glove box, is not shown to scale. The sample cell thickness in the transmission path is 2 cm.*

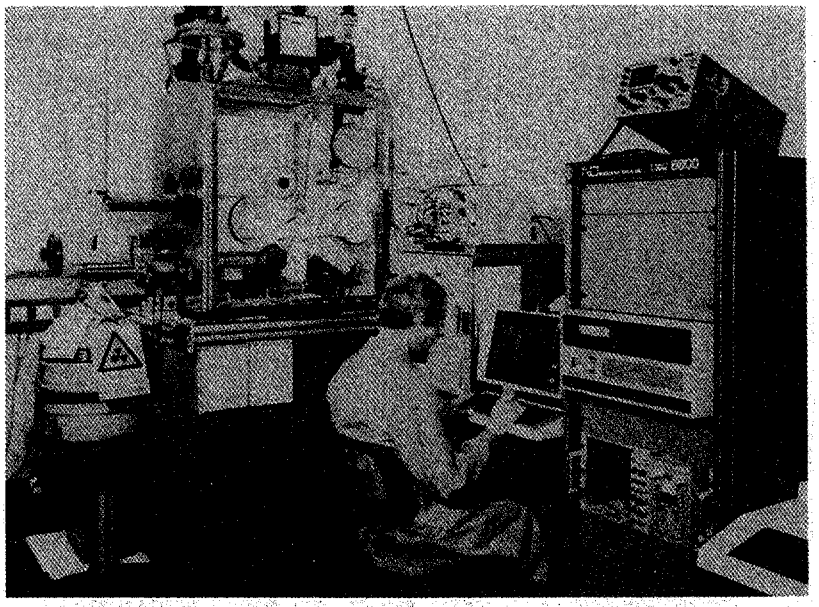

***Fig. 9.18** The KfK K-edge densitometer evaluated under the FRG support program to the IAEA.*

9.7.2 L_{III}-Absorption-Edge Densitometers

Given below are descriptions of several L_{III}-edge densitometers that have been tested and evaluated under actual or simulated in-plant environments. The first three L_{III}-edge densitometers described were designed to be equivalent, mechanically and electronically. Figure 9.19, a photograph of the AGNS instrument, represents all three instruments; Figure 9.20 is a line drawing of the measurement head for all three instruments. Table 9-5 summarizes the performance data for the instruments.

1. Savannah River Laboratory (SRL) (Refs. 12, 21, and 34). The L_{III}-edge densitometer at the Savannah River Laboratory was tested in conjunction with a solution coprocessing demonstration facility. The stainless steel flow-through solution sample cell (fitted with plastic windows) was plumbed into the glove box that housed the coprocessing setup, so that solution from various points in the process could be introduced into the cell for L_{III}-edge assay of either uranium or plutonium or both. The instrument measured 15-mL static solutions in the cell; before each assay, the instrument was flushed several times with the solution. The assay precisions obtained for pure uranium or plutonium solutions are plotted versus concentration in Figure 9.21. The instrument operated at Savannah River from 1978 until 1980.

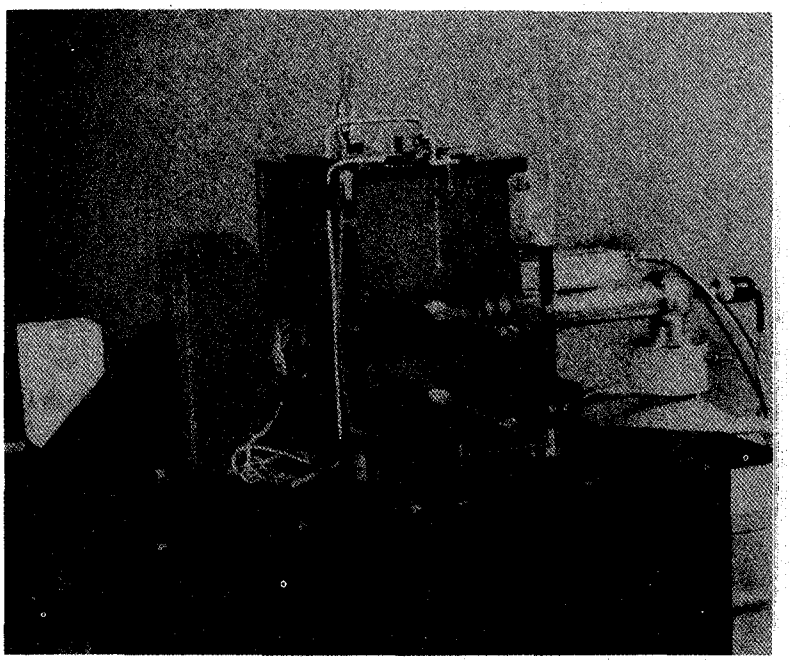

Fig. 9.19 *The AGNS L_{III}-edge densitometer. Shown (left to right) are the electronics inside an environmental enclosure, the measurement station, and the hard-copy terminal.*

2. New Brunswick Laboratory (NBL) (Ref. 35). The L_{III}-edge densitometer at the US Department of Energy New Brunswick Laboratory at Argonne was designed to reproduce the measurement geometry and assay method of the Savannah River Laboratory instrument. Prepared reference solutions of uranium, plutonium, and mixed solutions were used in a carefully controlled evaluation of the precision and accuracy of this instrument. The NBL assay results are compared with reference values for pure uranium solutions in Figure 9.22. The sensitivity to matrix contaminants with low-, intermediate-, and high-Z elements was examined for contamination levels up to 10% (of SNM) by weight. This evaluation took place from 1980 to 1981.

3. Allied General Nuclear Services (AGNS) (Ref. 36). An L_{III}-edge densitometer designed to perform continuous assays of uranium concentration in flowing process streams was tested in 1981 at the AGNS Barnwell facility. The stainless steel flow-through cell was plumbed into a line that continuously sampled the product stream of a solvent extraction column. The instrument operated for seven days without interruption, providing uranium concentration results every 5 min, analyzing flowing solutions

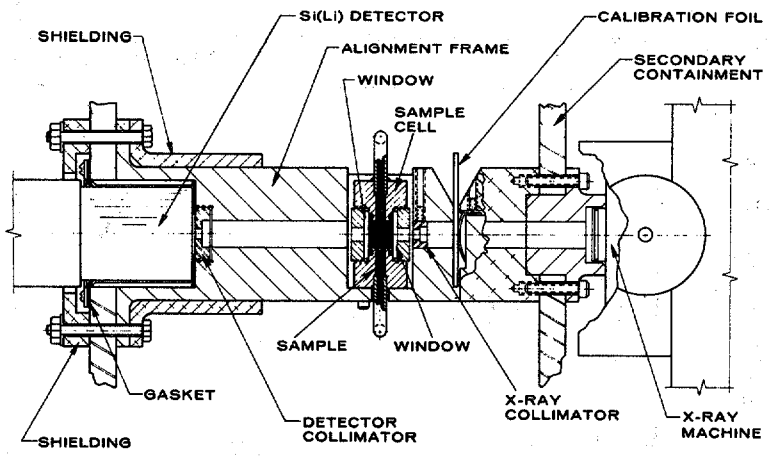

Fig. 9.20 *Scale line drawing of the L_{III}-edge densitometer measurement head for the SRL, NBL, and AGNS instruments. The flow-through sample cell is shown cut off at the inlet and outlet tubes. The darkened area indicates the solution in the cell (1-cm transmission path length). The materials for secondary containment, shielding, frame, sample cell, and collimator are polycarbonate (Lexan™), stainless steel, aluminum, stainless steel (with Kel-F™ windows), and brass, respectively.*

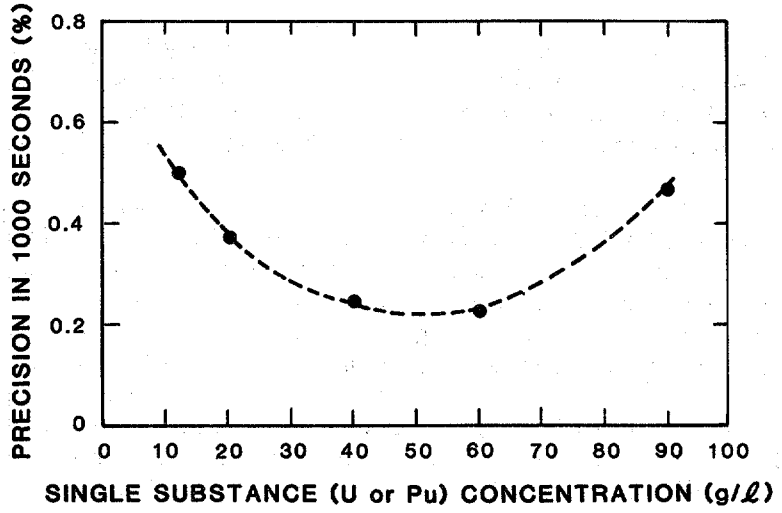

Fig. 9.21 *Precision (1σ) measured at SRL for 1000-s L_{III}-edge assays of uranium or plutonium plotted versus concentration. The dashed line is the calculated standard deviation, based on counting statistics, using Equation 9-14.*

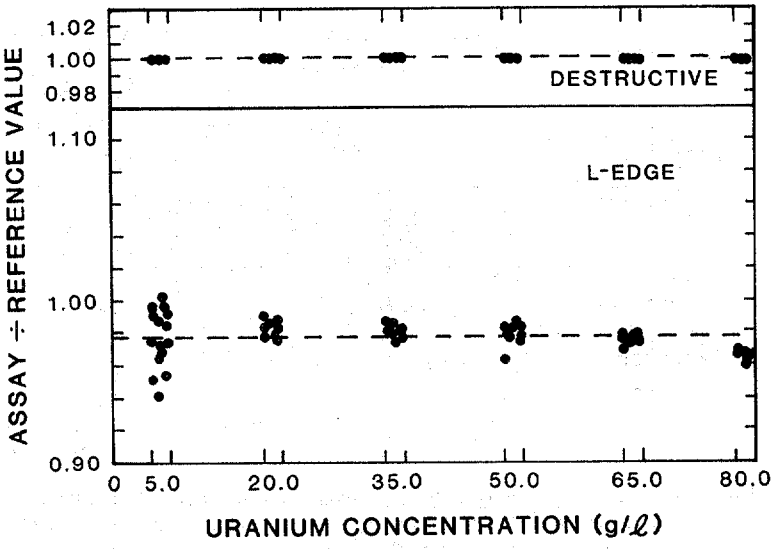

Fig. 9.22 Comparison of single 1000-s L_{III}-edge assays and destructive analysis of solution samples introduced into the sample cell of the NBL instrument. Groups of three data points plotted vertically represent repeated assays of the same sample. These data were used to establish the calibration of the NBL instrument.

from startup (essentially zero uranium concentration) to steady-state levels of approximately 40 g/L. The instrument provided a hard copy of the near-real-time results automatically to a materials control and accounting computer programmed to draw near-real-time material balances using readouts from process monitoring equipment.

4. Los Alamos National Laboratory (Ref. 37). A compact L_{III}-edge densitometer was tested in 1984 at Los Alamos in the Group Q-1 Safeguards Laboratory. This instrument used a commercial x-ray generator designed for portable applications. Figure 9.23 shows the measurement head. Although a standard rack of electronics was employed for analog signal processing and for data acquisition and analysis, the portable multichannel analyzer used in the compact K-edge densitometer at Seibersdorf (see Section 9.7.1) could have been employed in the L-edge densitometer at Los Alamos, allowing portable applications to be considered for L_{III}-edge measurements. The performance of the compact densitometer with prepared reference solutions of uranium was equal to that of the L_{III}-edge instruments tested previously.

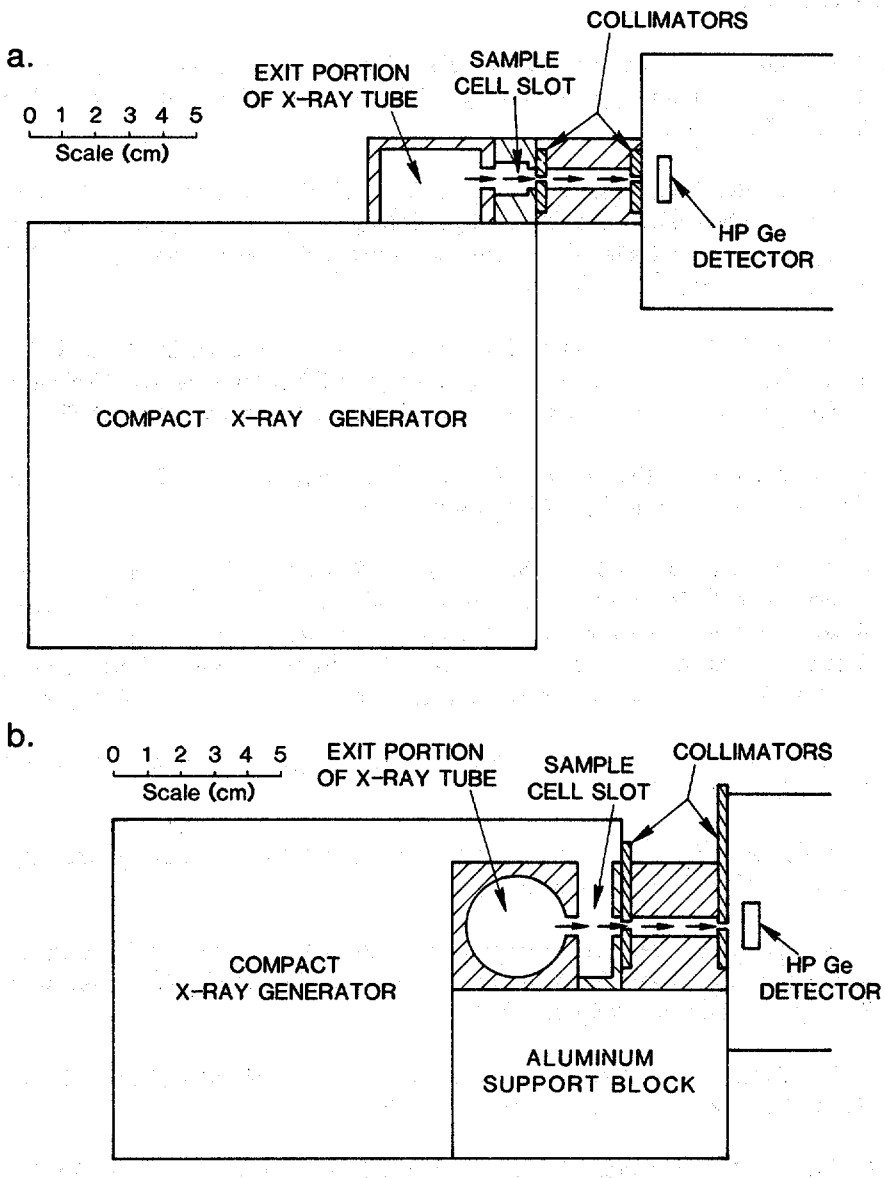

Fig. 9.23 *Scale line drawings of the compact L_{III}-edge densitometer measurement head: (a) view from above in the horizontal plane of the x-ray transmission path; (b) side view. The solution thickness in the trasmission path is 1 cm.*

REFERENCES

1. T. R. Canada, J. L. Parker, and T. D. Reilly, "Total Plutonium and Uranium Determination by Gamma-Ray Densitometry," *Transactions of the American Nuclear Society* 22, 140 (1975).

2. T. R. Canada, D. G. Langner, and J. W. Tape, "Nuclear Safeguards Applications of Energy-Dispersive Absorption-Edge Densitometry," in *Nuclear Safeguards Analysis*, E. A. Hakkila, Ed. (American Chemical Society, Washington, DC, 1978), Series No. 79, p. 96.

3. T. R. Canada, S. -T. Hsue, D. G. Langner, D. R. Martin, J. L. Parker, T. D. Reilly, and J. W. Tape, "Applications of the Absorption-Edge Densitometry Technique to Solutions and Solids," *Nuclear Materials Management* 6 (3), 702 (1977).

4. R. L. Bramblett, "Passive and Active Measurements of SNM in 55-Gallon Drums," *Nuclear Materials Management* 4, 137 (1975).

5. H. A. Smith, Jr., T. Marks, S. S. Johnson, L. R. Cowder, J. K. Sprinkle, Jr., C. O. Shonrock, R. W. Slice, D. L. Garcia, K. W. MacMurdo, R. L. Pollard, L. B. Baker, P. Christie, and J. P. Clark, "Test and Evaluation of the In-Line Plutonium Solution K-Absorption-Edge Densitometer at the Savannah River Plant: Phase I, Off-Line Testing," Los Alamos National Laboratory report LA-9124-MS (1982).

6. S. -T. Hsue to R. B. Walton, "Densitometry Design," Los Alamos document Q-1-80-243 (May 1980).

7. L. A. Currie, "Limits for Quantitative Detection and Quantitative Determination," *Analytical Chemistry* 40, 586 (1968).

8. C. E. Crouthamel et al., "A Compilation of Gamma-Ray Spectra (NaI Detector)," in *Applied Gamma-Ray Spectrometry*, F. Adams and R. Dams, Eds. (Pergamon Press, Braunschweig, Hungary, 1970).

9. T. W. Crane, "Detectability Limits and Precision for Shufflers," Los Alamos National Laboratory report LA-10158-MS (1984).

10. E. Storm and H. I. Israel, "Photon Cross Sections from 0.001 to 100 MeV for Elements 1 through 100," Los Alamos Scientific Laboratory report LA-3753 (1967).

11. *Handbook of Chemistry and Physics*, 55th ed., R. C. Weast, Ed. (Chemical Rubber Company Press, Cleveland, Ohio, 1975).

12. P. A. Russo, S. -T. Hsue, D. G. Langner, and J. K. Sprinkle, Jr., "Nuclear Safeguards Applications of Energy-Dispersive Absorption-Edge Densitometry," *Nuclear Materials Management* 9, 730 (1981).

13. F. Brown, D. R. Terry, J. B. Hornsby, R. G. Monk, F. Morgan, J. Herrington, P. T. Good, K. C. Steed, and V. M. Sinclair, "Application of Instrumental Methods to the Determination of Nuclear Fuel Materials for Safeguards," in *Safeguards Techniques*, Proc. IAEA Karlsruhe Symp. (IAEA, Vienna, Austria, July 1970), Vol. II, p. 125.

14. D. R. Terry and A. P. Dixon, "A Portable Gamma Absorptiometer for Safeguards Use in Nuclear Fuel Reprocessing Plants," Atomic Weapons Research Establishment report AWRE/44/88/28 Cos 28, Aldermaston, England (1975).

15. J. E. Ayer and D. R. Schmitt, "A Gamma-Ray Absorptiometer for Nuclear Fuel Evaluation," *Nuclear Technology* 27, 442 (1975).

16. T. Gozani, H. Weber, and Y. Segal, "A Gamma-Ray Transmission Gauge for Determination of Heavy and Light Metal Loading of Fuel Elements," *Nuclear Materials Management* 2 (3), 139 (1973).

17. T. Gozani, *Active Nondestructive Assay of Nuclear Materials, Principles and Applications*, NUREG/CR-0602, (US Nuclear Regulatory Commission, Washington DC, 1981), p. 118.

18. G. Bardone, M. Aparo, and F. V. Frazzoli, "Dual-Energy X-Ray Absorptiometry for the Assay of Mixed Special Nuclear Material in Solution," in *Proc. Second Annual Symposium on Safeguards and Nuclear Materials Management*, Edinburgh, Scotland, March 26-28, 1980 (European Safeguards Research and Development Association, Brussels, Belguim, 1980), p. 270.

19. M. Aparo, B. Mattia, F. V. Frazzoli, and P. Zeppa, "Dual-Energy X-Ray Absorptiometer for Nondestructive Assay of Mixed Special Nuclear Material in Solution," in *Proc. Fifth Annual Symposium on Safeguards and Nuclear Materials Management*, Versailles, France, April 19-21, 1983 (European Safeguards Research and Development Association, Brussels, Belgium, 1983), p. 271.

20. J. K. Sprinkle, Jr., H. R. Baxman, D. G. Langner, T. R. Canada, and T. E. Sampson, "The In-Plant Evaluation of a Uranium NDA System," in *Proc. American Nuclear Society Topical Conference on Measurement Technology for Safeguards and Materials Control*, Kiawah Island, South Carolina, November 26-28, 1979 (National Bureau of Standards, Washington, DC, 1980), p. 324.

21. T. R. Canada, J. L. Parker, and P. A. Russo, "Computer-Based In-Plant Nondestructive Assay Instrumentation for the Measurement of Special Nuclear Materials," in *Proc. American Nuclear Society Topical Conference on Computers in Activation Analysis in Gamma-Ray Spectroscopy*, Mayaguez, Puerto Rico. April 30-May 4, 1978 (US DOE Technical Information Center), p. 746.

22. H. H. Hogue and S. E. Smith, "Off-Line Nondestructive Analysis at a Uranium Recovery Facility," in *Safeguards Technology: The Process-Safeguards Interface*, Proc. American Nuclear Society-INMM Topical Conference, Hilton Head Island, South Carolina, November 28-December 2, 1983 (Conf. 831106, 1984).

23. H. H. Hogue and S. E. Smith, "Nondestructive Analysis at the Oak Ridge Y-12 Plant," Oak Ridge Y-12 Plant report Y-2297 (1984).

24. K. J. Hofstetter, G. A. Huff, R. Gunnink, J. E. Evans, and A. L. Prindle, "On-Line Measurement of Total and Isotopic Plutonium Concentrations by Gamma-Ray Spectrometry," in *Analytical Chemistry in Nuclear Fuel Reprocessing*, W. S. Lyon, Ed. (Science Press, Princeton, New Jersey, 1978), p. 266, and University of California report UCRL-52220 (1977).

25. K. J. Hofstetter and G. A. Huff, "On-Line Isotopic Concentration Monitor," Allied General Nuclear Services report AGNS-1040-2.3-52 (1978).

26. L. R. Cowder, S. -T. Hsue, S. S. Johnson, J. L. Parker, P. A. Russo, J. K. Sprinkle, Jr., Y. Asakura, T. Fukuda, and I. Kondo, "An Instrument for the Measurement of Pu Concentration and Isotopics of Product Solutions at Tokai-Mura," in *Proc. Second Annual Symposium on Safeguards and Nuclear Materials Management*, Edinburgh, Scotland, March 26-28, 1980 (European Safeguards Research and Development Association, Brussels, Belgium, 1980), p. 119.

27. P. A. Russo, S. -T. Hsue, J. K. Sprinkle, Jr., S. S. Johnson, Y. Asakura, I. Kondo, J. Masui, and K. Shoji, "In-Plant Measurements of Gamma-Ray Transmissions for Precise K-Edge and Passive Assay of Plutonium Concentration and Isotopic Fractions in Product Solutions," Los Alamos National Laboratory report LA-9440-MS (1982).

28. Y. Asakura, I. Kondo, J. Masui, K. Shoji, P. A. Russo, S. -T. Hsue, J. K. Sprinkle, Jr., and S. S. Johnson, "In-Plant Measurements of Gamma-Ray Transmissions for Precise K-Edge and Passive Assay of Plutonium Concentration and Isotopic Abundances in Product Solutions at the Tokai Reprocessing Plant," *Nuclear Materials Management* 11, 221 (1982).

29. H. A. Smith, Jr., T. Marks, L. R. Cowder, C. O. Shonrock, S. S. Johnson, R. W. Slice, J. K. Sprinkle, Jr., K. W. MacMurdo, R. L. Pollard, and L. B. Baker, "Development of In-Line Plutonium Solution NDA Instrumentation at the Savannah River Plant," in *Proc. Second Annual Symposium on Safeguards and Nuclear Materials Management*, Edinburgh, Scotland, March 26-28, 1980 (European Safeguards Research and Development Association, Brussels, Belgium, 1980), p. 123.

30. L. R. Cowder, S. F. Klosterbuer, R. H. Augustson, A. Esmailpour, R. Hawkins, and E. Kuhn, "A Compact K-Edge Densitometer," in *Proc. Sixth Annual Symposium on Safeguards and Nuclear Materials Management*, Venice, Italy, May 14-18, 1984 (European Safeguards Research and Development Association, Brussels, Belgium, 1984), p. 261.

31. H. Eberle, P. Matussek, H. Ottmar, I. Michel-Piper, M. R. Iyer, and P. P. Chakraborty, "Nondestructive Elemental and Isotopic Assay of Plutonium and Uranium in Nuclear Materials," Nuclear Safeguards Technology 1978 (International Atomic Energy Agency, Vienna, Austria, 1979), Vol. II, p. 27.

32. H. Eberle, P. Matussek, I. Michel-Piper, and H. Ottmar, "Assay of Uranium and Plutonium in Solution by K-Edge Photon Absorptiometry Using a Continuous X-Ray Beam," in *Proc. Second Annual Symposium on Safeguards and Nuclear Materials Management*, Edinburgh, Scotland, March 26-28, 1980 (European Safeguards Research and Development Association, Brussels, Belgium, 1980), p. 372.

33. H. Eberle, P. Matussek, I. Michel-Piper, and H. Ottmar, "Operational Experience with K-Edge Photon Absorptiometry for Reprocessing Feed and Product Solution Analysis," in *Proc. Third Annual Symposium on Safeguards and Nuclear Materials Management*, Karlsruhe, Fed. Rep. Germany, May 6-8, 1981 (European Safeguards Research and Development Association, Brussels, Belgium, 1981), p. 109.

34. P. A. Russo, T. R. Canada, D. G. Langner, J. W. Tape, S. -T. Hsue, L. R. Cowder, W. C. Moseley, L. W. Reynolds, and M. C. Thompson, "An X-Ray L_{III}-Edge Densitometer for Assay of Mixed SNM Solutions," in *Proc. First Annual Symposium on Safeguards and Nuclear Materials Management*, Brussels, Belgium, April 25-27, 1979 (European Safeguards Research and Development Association, Brussels, Belgium, 1979), p. 235.

35. W. J. McGonnagle, M. K. Holland, C. S. Reynolds, N. M. Trahey, and A. C. Zook, "Evaluation and Calibration of a Los Alamos National Laboratory L_{III}-Edge Densitometer," US Department of Energy New Brunswick Laboratory report NBL-307 (1983).

36. P. A. Russo, T. Marks, M. M. Stephens, A. L. Baker, and D. D. Cobb, "Automated On-Line L-Edge Measurement of SNM Concentration for Near-Real-Time Accounting," Los Alamos National Laboratory report LA-9480-MS (1982).

37. M. L. Brooks, P. A. Russo, and J. K. Sprinkle, Jr., "A Compact L-Edge Densitometer for Uranium Concentration Assay," Los Alamos National Laboratory report LA-10306-MS (1985).